

# 中国激光

## 基于表面等离子体共振的高灵敏度光纤微流控芯片

李钢敏, 李致远, 李正冉, 王锦民, 夏历\*, 杨墨, 李微

华中科技大学光学与电子信息学院, 湖北 武汉 430074

**摘要** 设计了一种可嵌入基于表面等离子体共振(SPR)光纤传感器的微流控芯片, 可用于溶液浓度的测量。采用具有良好化学惰性的有机聚合材料聚二甲基硅氧烷(PDMS)作为芯片主体的制作材料, 在芯片中微流控通道内采用镀有 60 nm 金膜的多模光纤-光子晶体光纤-多模光纤(MMF-PCF-MMF)传感结构来激发 SPR 效应。当注入微流体通道的溶液浓度发生变化时, 由于光纤传感部分外部折射率的变化引起 SPR 谐振谷移动, 故该芯片可用于测量溶液浓度。本芯片微流控通道直径为 0.2 mm, 最高检测灵敏度可达 8240.6 nm/RIU, 具有便于实时测量、高灵敏度、高可靠性、溶液用量少等特点。

**关键词** 光纤光学; 光纤传感器; 光子晶体光纤; 表面等离子体共振; 微流控芯片

中图分类号 TP212.1 文献标志码 A

doi: 10.3788/CJL202148.0106002

### 1 引言

光纤表面等离子体共振(SPR)技术作为一种近代物理光学、材料化学等学科交叉结合的新兴传感技术, 具有免标记、预处理简单、分析快速、高灵敏等优良特性, 逐渐在食品安全、环境监测等众多领域中得到广泛使用<sup>[1-3]</sup>, 目前国内外已研制出多种基于 SPR 的浓度传感器。吉林大学高璐等<sup>[4]</sup>设计了一种基于 Kretschmann 型棱镜的 SPR 原理折射率检测实验系统, 通过 MATLAB 仿真得到其理论检测灵敏度为 6049 nm/RIU( RIU 为单位折射率), 实际检测出来的实验结果与仿真结果近似相等。然而基于 Kretschmann 型棱镜型的 SPR 传感器体积庞大, 需配备机械可动部件, 不利于器件小型化和远程传感。光纤 SPR 传感器凭借其体积小、结构紧凑以及可实现远程测量的优势, 越来越受到研究人员的广泛关注。南京信息工程大学蔡凯杰<sup>[5]</sup>设计并制作了一种基于 D 型光纤的 SPR 传感器, 在介质折射率 1.33~1.39 范围内, 基于金膜激励 SPR 效应时灵敏度达 2851 nm/RIU, 基于银膜时灵敏度更高, 达 3319 nm/RIU; 南京信息工程大学郭志勇等<sup>[6]</sup>设计了一种基于多模-单模-多模 (MSM) 结构的光纤折射率传感器, 并且在单模光纤

表面涂覆二氧化钛/银(TiO<sub>2</sub>/Ag)复合膜构成传感单元, Ag 膜厚度与 TiO<sub>2</sub> 膜厚度达到传感器性能最优条件时, 在 1.33~1.41 环境折射率范围内, 传感器灵敏度约为 6875 nm/RIU。基于上述方法研制的光纤 SPR 折射率传感器, 虽然灵敏度较高, 但大多未考虑传感监测过程中样品的消耗量, 且裸露的光纤易碎, 传感器的稳定性不足。

微流控芯片系统作为高通量微尺度分析设备, 近年来在环境检测、远距离监控、生物检测等多种领域展现出巨大的潜力<sup>[7]</sup>。本研究将光纤 SPR 与微流控通道相结合, 形成简单的微型化系统, 大幅减少了样品消耗量, 并将传感光纤部分嵌入有机聚合材料聚二甲基硅氧烷(PDMS)基片, 以防止其受到损坏而对传感器稳定性造成影响, 同时使用光子晶体光纤(PCF)与多模光纤(MMF)熔接而成的异芯结构作为传感部分, 在传感结构表面镀 60 nm 厚的金膜, 以激励 SPR 效应。其中, PCF 是近年来出现的一种新型光纤, 这种光纤通常由单一电介质构成, 其微结构包层由二维方向上紧密排列而在轴向结构不变的波长量级空气孔组成, 具有独特的导光特性, 能够激发更强的 SPR 效应<sup>[8-9]</sup>。本文所提出的传感器的最高检测灵敏度为 8240.6 nm/RIU, 在灵敏度方面有

收稿日期: 2020-06-15; 修回日期: 2020-07-17; 录用日期: 2020-08-20

基金项目: 国家自然科学基金(61775065)、大学生创新创业训练计划项目(2020104870005)

\*E-mail: xiali@hust.edu.cn

较大提升,另外微流控芯片具有体积小、结构轻便、便于携带、性能稳定等特点,即使在非实验室环境下测量仍具有较高准确度与可靠性,不易受环境的影响。

## 2 基本原理与实验过程

### 2.1 基本原理

SPR 是金属表面存在的电荷密度波被激发并沿金属与介质表面传播的物理光学现象<sup>[10]</sup>。如图 1 所示,入射光在介质与金属薄膜的界面上发生内全反射时,会产生隐失波,当隐失波与表面等离子体波满足相位匹配条件时,会发生表面等离子体共振,使全反射能量降低<sup>[11]</sup>。将均匀厚度的金属薄膜镀于传感光纤外表面以激励 SPR 效应,并在出射端利用光谱仪进行光谱检测,获得传感区发生 SPR 时的对应光波长,进而确定液体的折射率。

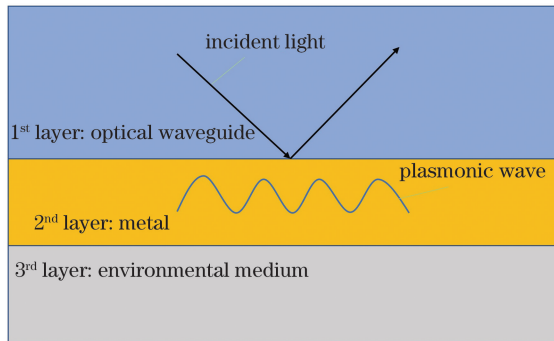


图 1 表面等离子共振原理图

Fig. 1 Schematic diagram of surface plasmon resonance

当入射光波的入射角固定时,发生共振的入射光频率与待测溶液的折射率相关。对于基于光子晶体光纤的表面等离子共振,只有水平方向的分量起作用。假定光波波矢  $k$  在  $x$  轴方向的分量大小  $k_x$  为<sup>[11-12]</sup>

$$k_x = \frac{\omega}{c} \sqrt{\xi_0(\lambda) \sin \theta}, \quad (1)$$

其中  $\omega$  为入射光的角频率,  $c$  为光速,  $\theta$  为可见光的

入射角,  $\xi_0(\lambda)$  为纤芯的介电常数。金属和介质表面的等离子体波的波矢大小  $k_{sp}$  可以表示为

$$k_{sp} = \frac{\omega}{c} \sqrt{\frac{\xi_1(\lambda) \xi_m(\lambda)}{\xi_1(\lambda) + \xi_m(\lambda)}}, \quad (2)$$

其中  $\xi_1(\lambda)$  为待测液体的介电常数,  $\xi_m(\lambda)$  为金属介质的介电常数。由(1)式和(2)式可以看出,入射光波长、纤芯的介电常数、入射角度、待测溶液的介电常数以及金属介质的介电常数等因素都会影响入射光波与等离子体的相位匹配。当  $k_{sp} = k_x$  时,等离子体模式与纤芯导模模式满足相位匹配条件,产生的等离子共振效应最强,对应的共振角度为

$$\sin \theta = \sqrt{\frac{\xi_1(\lambda) \xi_m(\lambda)}{\xi_0(\lambda) [\xi_1(\lambda) + \xi_m(\lambda)]}}. \quad (3)$$

当宽带光源以一定角度入射光纤时,可通过检测输出光谱的特性曲线得到吸收峰对应的光波长。普通光纤用作传感光纤时存在耦合损耗大、保偏性差等缺点,限制了 SPR 传感器器性能的进一步提高<sup>[13]</sup>,而 PCF 可以通过向纤芯中引入中空微结构来降低模式折射率,因此可以方便地实现纤芯模和表面等离子模的相位匹配,获得更宽的检测范围和更高的分辨率<sup>[6]</sup>。本文所提出的 PCF 结构及其包层模式的光场能量分布如图 2 所示。图 2(a) 为正六边形实芯 PCF, 空气孔孔径和相邻不同层空气孔间距分别为  $3.5 \mu\text{m}$  和  $7.0 \mu\text{m}$ , 第一层实芯直径为  $14 \mu\text{m}$ , 光纤外边缘镀有一层  $60 \text{ nm}$  金膜, 光纤置于折射率液体环境中, 并在最外层设置一层厚约  $5 \mu\text{m}$  的完美匹配层(PML)用于数值分析。在 COMSOL 中进行数值分析, 模拟波长设置为  $850 \text{ nm}$ , 将液体、PCF 空气孔和 PCF 包层的折射率分别设置为  $1.3380$ 、 $1.4509$  和  $1.000$ , 金膜的折射率设为  $0.2438 + 4.9346i$ 。在多模干涉结构中, 主要强调传感光纤中包层模式对 SPR 的激励作用, 因此在分析中模拟了 PCF 中包层模式的模态分布情况。仿真结

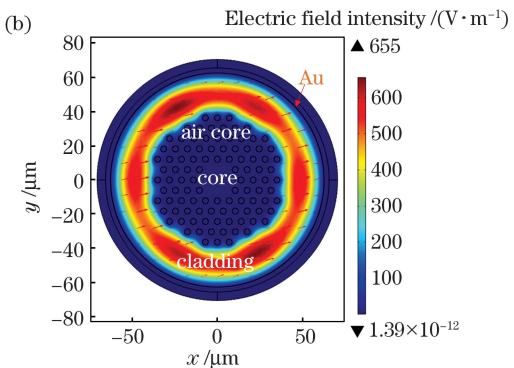


图 2 仿真结果。(a)光子晶体光纤结构图 ;(b)包层模式的光场能量分布图

Fig. 2 Simulation results. (a) Schematic diagram of PCF; (b) light field energy distribution of the cladding mode

果表明,PCF气孔外侧的二氧化硅包层形成高折射率环,使得高阶包层模式的能量集中在金膜附近,如图2(b)所示。因此,PCF可以激发较强的SPR效应,提高传感器的折射率传感能力。

## 2.2 传感结构制作

光纤传感结构是由两段MMF与一段长约10 mm的PCF熔接而成的多模干涉结构。制成的传感光纤结构如图3所示,两端的MMF的纤芯和包层直径分为 $105\text{ }\mu\text{m}$ 和 $125\text{ }\mu\text{m}$ ,用作传输波导。光纤结构中间的异芯光纤选择正六边形实芯PCF,

其纤芯直径和包层直径大小分别为 $20\text{ }\mu\text{m}$ 和 $125\text{ }\mu\text{m}$ ,空气孔孔径大小为 $3.5\text{ }\mu\text{m}$ ,相邻空气孔间距为 $7.0\text{ }\mu\text{m}$ ,用作SPR传感能区。

图4为在扫描电子显微镜(SEM)下的光纤结构剖面图。PCF剖面图如图4(a)所示。使用电阻式蒸发镀膜机在熔接而成的MMF-PCF-MMF传感光纤结构表面镀一层厚度约为 $60\text{ nm}$ 、适合激发SPR的金膜,如图4(b)所示。最后,在已经镀膜的MMF-PCF-MMF结构两端熔接带有接头的同规格多模光纤,便于进行实验测量。

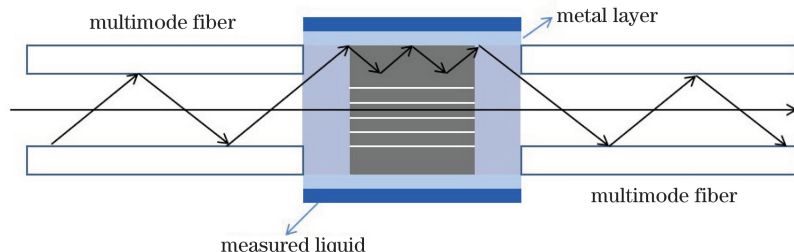


图3 传感光纤结构示意图

Fig. 3 Schematic diagram of sensing optical fiber structure

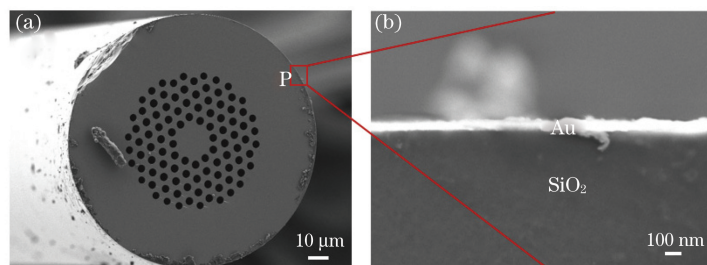


图4 光子晶体光纤结构图。(a)光子晶体光纤的SEM剖面图;(b)PCF边界上的位置缩放图

Fig. 4 Structure diagram of photonic crystal fiber. (a) SEM profile of PCF; (b) zoom on PCF

## 2.3 芯片设计

本课题组所设计的光纤SPR芯片结构如图5所示。微流控芯片设计成长方体结构,长为5 cm,宽为3.5 cm,厚度为1 cm,结构底部中间含有与芯片长边平行的微流控通道,其直径为 $200\text{ }\mu\text{m}$ ,长度与芯片长度相同。光纤从芯片底部中央主通道穿过,传感部分位于芯片中间。为了防止注射溶液的

针孔插入芯片时对传感部分造成损伤,在距离芯片前后边缘1 cm处分别从中间微流控通道延伸出一条长度为0.5 cm、截面与主通道同等大小且垂直于中间主通道的支通道,分别向左右两边延伸,用作待测溶液的进出口通道。

芯片的制作材料选用具有良好化学惰性的可塑形有机材料PDMS。制作时首先将主剂与固化剂以

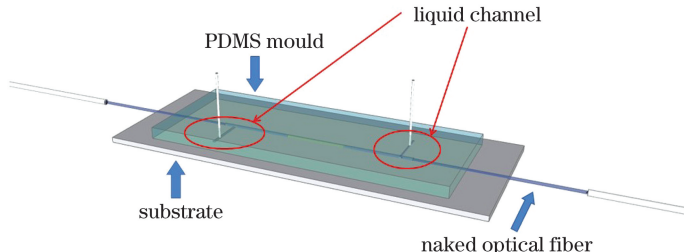


图5 微流控芯片结构图

Fig. 5 Structure diagram of microfluidic chip

10:1混合均匀,缓缓倒入3D打印而成的树脂模具中。将倒满混合胶体的3D模具置于通风处1~2 d,待其PDMS胶体静置凝固,切割取出PDMS芯片。最后将事先制作完成的传感光纤置于PDMS芯片上预留的微流控通道中,并与玻璃片稳定键合。

## 2.4 实验过程

实验装置如图6所示。实验系统由HL-2000卤钨光源、嵌入光纤SPR结构的微流控芯片、烧杯、导管、注射泵,光纤光谱仪USB4000及计算机组成。注射泵匀速地将注射器中的葡萄糖溶液注入微流控芯片,流经光纤传感部分,最后进入废液缸,由卤钨

灯产生的光源经光纤耦合进入SPR传感器,由于传感光纤具有隐失场,满足共振条件的光波将激发金膜产生表面等离子体共振,在透射光上产生共振谷,用微型光谱仪采集、记录透射光谱并传输给计算机。折射率不同会导致共振谷的位置移动,通过记录系列样品的共振光谱,定标传感器对折射率的传感特性。在室温条件下(25℃),将不同质量的葡萄糖固体样品与去离子水以一定比例混合作为待测样品,该混合溶液的折射率在1.338~1.425之间。传感光纤结构部分用金膜厚度为60 nm的PCF-SPR进行测试。

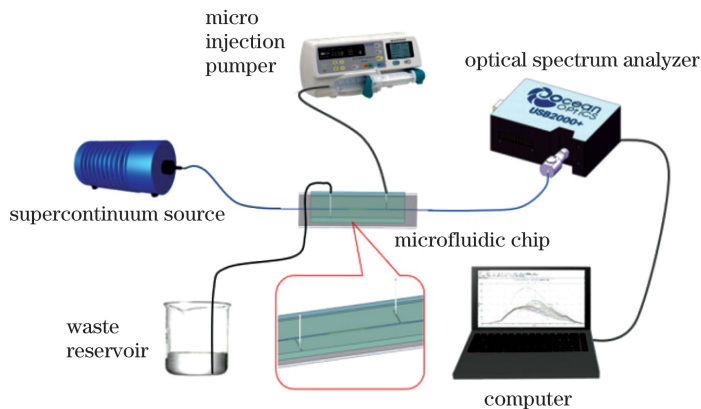


图6 实验装置图

Fig. 6 Experimental setup

## 3 分析与讨论

在上述实验条件下得到的SPR光谱曲线如图7(a)所示,插图为电子显微镜下PCF与MMF的熔接结构图。当待测液的折射率由1.338逐渐增大到1.425时,SPR光谱的共振波长位置向长波长方向漂移。对于内置传感光纤的微流控芯片,光线经过传感区时会有明显的吸收,最大的吸收波长与浓

度相关,且溶液折射率变化量在 $10^{-3}$ 量级时,谱线最小值位置有显著偏移,故该类微流控芯片具有高灵敏度的优良特性。提取待测液的折射率与共振波长的关系,并以 $n=1.338$ 时的共振波长为起始点,根据实验测试结果绘制得到图7(b)。曲线上升速度与芯片灵敏度相关,上升越快,灵敏度越高。结果表明PCF-SPR传感器折射率灵敏度可高达8240.6 nm/RIU,符合高灵敏度的应用需求。

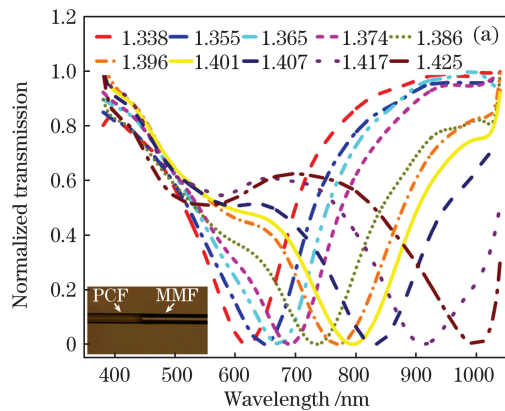


图7 实验结果。(a)基于PCF-SPR传感器的归一化透射光谱;

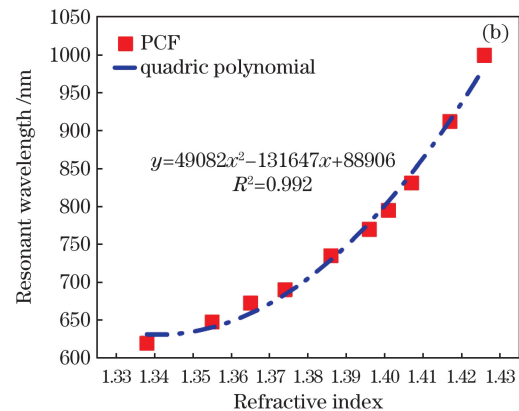


Fig. 7 Experimental results. (a) Normalized transmission spectra of PCF-SPR sensors; (b) relationship between resonant wavelength and refractive index of PCF-SPR structure

## 4 结 论

基于等离子体共振的光纤结构设计制造了一种新型的微流控芯片 SPR 传感器, 体积为  $3.5\text{ cm} \times 1\text{ cm} \times 5\text{ cm}$ , 远小于传统的测量仪器。通过对基于表面等离子体共振的光子晶体光纤结构进行测试, 在  $1.338\sim1.425$  的宽折射率测量范围内获得了高达  $8240.6\text{ nm/RIU}$  的传感器灵敏度。该结构因其具有良好的折射率灵敏度, 小巧的体积以及耐酸、抗腐蚀能力, 将在生物化学领域具有更广阔的应用前景。

## 参 考 文 献

- [1] Sun D F, Liu P. Solution concentration measurement system based on optical fiber spectrometer [J]. Physical Experiment of College, 2019, 32(3): 82-85.
- [2] Wang Q. The preparation and properties of optical fiber sensor based on surface plasmon resonance [D]. Nanjing: Nanjing University of Posts and Telecommunications, 2019: 1-3.
- [3] Zhao J, Wang Y, Wang Y P. Graphene-oxide-enhanced surface plasmon resonance fiber sensor [J]. Laser & Optoelectronics Progress, 2019, 56(23): 230601.
- [4] Gao L, Gao W Z, Luo Z C, et al. SPR principle refractive index testing system for offshore oil spill [J]. Infrared and Laser Engineering, 2019, 48(8): 0813006.
- [5] Cai K J. Research on surface plasmon resonance refractive index sensor based on D-type optical fiber [D]. Nanjing: Nanjing University of Information Science & Technology, 2019: 9-12.
- [6] Guo Z Y, Ge Y X, Shen L W, et al. Surface plasmon resonance fiber refractive index sensor based on MSM structure [J]. Semiconductor Optoelectronics, 2020, 41(2): 205-210.
- [7] Li C H, Ma Z C, Hu X Y, et al. Preparation and application of microfluidic Raman detection chip [J]. Chinese Journal of Lasers, 2021, 48(1): 0100001.
- [8] Xiao G L, Zhang K F, Yang H Y, et al. Refractive index sensor with double resonance peaks for D-type symmetric two-core photonic crystal fiber [J]. Acta Optica Sinica, 2020, 40(12): 1206001.
- [9] Liu H, Bai B B, Zhang Y Z, et al. High-sensitivity temperature measurement based on SPR in gold-PDMS-coated photonic crystal fiber [J]. Chinese Journal of Lasers, 2020, 47(4): 0404003.
- [10] Chen Q H, Han W Y, Kong X Y, et al. Detection of solution refractive index variation based on optical fiber surface plasmon resonance [J]. Chinese Journal of Lasers, 2020, 47(8): 0804003.
- [11] Zheng Y B. Research on multi-core photonic crystal fiber laser and surface plasmon resonance sensor with photonic crystal fiber [D]. Tianjin: Tianjin University, 2012: 74-76.
- [12] Wang F C. Study of outer coated photonic crystal fiber based surface plasmon resonance sensor [D]. Qinhuangdao: Yanshan University, 2019: 19-22.
- [13] Fan Z K, Zhang Z C, Wang B Z, et al. Research progress of photonic crystal fiber refractive index sensors based on surface plasmon resonance effect [J]. Laser & Optoelectronics Progress, 2019, 56(7): 070004.
- [14] 范振凯, 张子超, 王保柱, 等. 基于表面等离子体共振效应的光子晶体光纤折射率传感器的研究进展 [J]. 激光与光电子学进展, 2019, 56(7): 070004.

郭志勇, 葛益娴, 沈令闻, 等. 基于 MSM 结构的表面等离子体共振光纤折射率传感器 [J]. 半导体光电, 2020, 41(2): 205-210.

[7] Li C H, Ma Z C, Hu X Y, et al. Preparation and application of microfluidic Raman detection chip [J]. Chinese Journal of Lasers, 2021, 48(1): 0100001.

李春赫, 马卓晨, 胡昕宇, 等. 微流控拉曼检测芯片的制备与应用 [J]. 中国激光, 2021, 48(1): 0100001.

[8] Xiao G L, Zhang K F, Yang H Y, et al. Refractive index sensor with double resonance peaks for D-type symmetric two-core photonic crystal fiber [J]. Acta Optica Sinica, 2020, 40(12): 1206001.

肖功利, 张开富, 杨宏艳, 等. D型对称双芯光子晶体光纤双谐振峰折射率传感器 [J]. 光学学报, 2020, 40(12): 1206001.

[9] Liu H, Bai B B, Zhang Y Z, et al. High-sensitivity temperature measurement based on SPR in gold-PDMS-coated photonic crystal fiber [J]. Chinese Journal of Lasers, 2020, 47(4): 0404003.

刘海, 白冰冰, 张砚曾, 等. 基于 SPR 效应的金-PDMS 涂覆光子晶体光纤高灵敏度温度测量 [J]. 中国激光, 2020, 47(4): 0404003.

[10] Chen Q H, Han W Y, Kong X Y, et al. Detection of solution refractive index variation based on optical fiber surface plasmon resonance [J]. Chinese Journal of Lasers, 2020, 47(8): 0804003.

陈强华, 韩文远, 孔祥锐, 等. 基于光纤表面等离子体共振检测溶液折射率变化 [J]. 中国激光, 2020, 47(8): 0804003.

[11] Zheng Y B. Research on multi-core photonic crystal fiber laser and surface plasmon resonance sensor with photonic crystal fiber [D]. Tianjin: Tianjin University, 2012: 74-76.

郑一博. 多芯光子晶体光纤激光器及光子晶体光纤表面等离子体共振传感研究 [D]. 天津: 天津大学, 2012: 74-76.

[12] Wang F C. Study of outer coated photonic crystal fiber based surface plasmon resonance sensor [D]. Qinhuangdao: Yanshan University, 2019: 19-22.

王福成. 外层镀膜光子晶体光纤表面等离子体共振传感器的研究 [D]. 秦皇岛: 燕山大学, 2019: 19-22.

[13] Fan Z K, Zhang Z C, Wang B Z, et al. Research progress of photonic crystal fiber refractive index sensors based on surface plasmon resonance effect [J]. Laser & Optoelectronics Progress, 2019, 56(7): 070004.

范振凯, 张子超, 王保柱, 等. 基于表面等离子体共振效应的光子晶体光纤折射率传感器的研究进展 [J]. 激光与光电子学进展, 2019, 56(7): 070004.

# High-Sensitivity Optical-Fiber Microfluidic Chip Based on Surface Plasmon Resonance

Li Gangmin, Li Zhiyuan, Li Zhengran, Wang Jinmin, Xia Li\*, Yang Zhao, Wei Li

*School of Optical and Electronic Information, Huazhong University of Science and Technology,  
Wuhan, Hubei 430074, China*

## Abstract

**Objective** Surface plasmon resonance (SPR) sensors based on Kretschmann prism are bulky and need to be equipped with mechanical movable parts, which is not conducive to the miniaturization and remote sensing of devices. Optical-fiber-based SPR technology has been widely used in food safety, environmental monitoring, and other fields owing to its label-free simple pretreatment, fast analysis, high sensitivity, and other excellent characteristics. However, most SPR sensors do not consider sample consumption in the process of sensor monitoring. The exposed optical fiber is fragile, which easily affects the sensor's stability. Highly sensitive optical fibers, such as tapered and D-shaped fibers, are vulnerable and unstable. In addition to the abovementioned problems, the sensitivity of existing SPR fiber sensors needs further improvement. As a high-throughput microscale analysis device, the microfluidic chip system has shown great potential in remote monitoring, biological detection, and other fields in recent years. In this paper, a microfluidic chip based on SPR fiber sensor is designed and used to measure the concentration of a solution. This chip has the advantages of small size, compact structure, and low sample consumption; it also reduces the fiber damage and effectively improves the sensing stability by embedding the sensing fiber into Polydimethylsiloxane (PDMS) substrate. Photonic crystal fiber (PCF) is a new type of optical fiber. PCF comprises a single dielectric, in which air holes are closely arranged in the two-dimensional direction but unchanged in the axial structure to form microstructure cladding. Moreover, it can stimulate a more substantial SPR effect for its unique light-guiding characteristics.

**Methods** In this paper, PDMS—which has good chemical inertia and good biocompatibility—is used as the main material to fabricate the microfluidic chip. After cooling and forming in 3D mold, PDMS is stably bonded with glass sheet to form the main structure of the chip. The microchip contains a microfluidic channel (diameter: 200 nm), whose length is the same as that of the chip. A sensing structure of multimode fiber-photonic crystal fiber-multimode fiber (MMF-PCF-MMF), which is coated with 60-nm gold film on the surface, is embedded in the channel to stimulate SPR effect. Then, mixed solutions of glucose solid sample and deionized water in a certain proportion with refractive index of 1.338–1.425 are used as samples to be tested. The experiment is performed at room temperature (25 °C). The glucose solution in the syringe is injected into the microfluidic chip using a syringe pump at a constant speed; the glucose solution flows through the optical fiber sensing part. When the concentration of the solution injected into the microfluidic chip is changed, the light wave meeting the resonance conditions excites the gold film to produce surface plasmon resonance and the resonant valley is generated on the transmitted spectrum. The position of the resonant valley shifts in the samples with different refractive indexes. By recording the resonance spectra of a series of samples, the sensitivity of the sensor with respect to the change in refractive index can be calibrated.

**Results and Discussions** When the refractive index of the liquid injected into the microfluidic chip increases from 1.338 to 1.425, the resonant wavelength of SPR spectrum shifts to longer wavelength because of the SPR resonance effect. The relationship between the refractive index and resonant wavelength of the liquid to be measured is extracted, and the sensitivity curve can be obtained by taking the resonant wavelength at  $n = 1.338$  as the starting point. The increasing speed of the sensitivity curve is related to the chip sensitivity. The experimental results show that the refractive index sensitivity of PCF SPR sensors can reach up to 8240.6 nm/RIU, in which RIU is refractive index unit, thereby showing that these have good high-sensitivity characteristics and meet the application requirements of high sensitivity.

**Conclusions** In this paper, a novel microfluidic chip embedded with SPR sensor is designed and manufactured by combining the optical fiber structure, SPR effect, and microfluidic system. The volume of chip is approximately 3.5 cm × 1 cm × 5 cm, which is much smaller than that of the traditional measurement instrument and is conducive to

the integration of sensor. After testing the MMF-PCF-MMF structure based on SPR effect, the sensor sensitivity obtained is high (up to 8240.6 nm/RIU) in a wide refractive index measurement range of 1.338–1.425. The proposed structure has good refractive sensitivity, small size, acid resistance, and corrosion resistance; these characteristics enable a broader application prospect in the field of biochemistry.

**Key words** fiber optics; fiber sensors; photonic crystal fibers; surface plasmon resonance; microfluidic chip

**OCIS codes** 060.2370; 060.5295; 240.6680